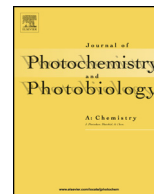Contents lists available at ScienceDirect

Journal of Photochemistry and Photobiology A: Chemistry

journal homepage: www.elsevier.com/locate/jphotochem

Short note

Photocatalytic degradation of methylene blue with copper(II) oxide synthesized by thermal decomposition of Flubendazole complexes

CrossMark

Ahmed M. Mansour*, Eslam M. El Bakry, Nour T. Abdel-Ghani*

Chemistry Department, Faculty of Science, Cairo University, Gamaa Street, Giza 12613, Egypt

ABSTRACT

Novel copper(II) complexes of an anti-parasitic Flubendazole drug (FLU), $[Cu(FLU)_2X_2]\cdot zH_2O$ (X = Cl^- (**1**), $C_2H_3O_2^-$ (**3**), and ClO_4^- (**4**), z = 1–4) and $[Cu(NO_3)(FLU)_2(OH_2)]\cdot NO_3\cdot 2H_2O$ (**2**) were synthesized and characterized using elemental analysis, TG, IR, EPR, magnetic and conductance measurements. Geometry optimization and natural bond orbital analysis were performed at DFT/B3LYP/6-31G* level of theory. Electronic transitions were calculated by TD-DFT. Tenorite (CuO) nanoparticles with promising catalytic properties were prepared in air via the controlled thermal decomposition of **1–4**. The polymorph and morphology of the prepared nano-tenorite particles were investigated by powder XRD and field emission scanning electron microscope. The catalytic degradation of methylene-blue (MB) dye exposed to the UV radiation in presence of CuO nanoparticles as a catalyst was studied at room temperature in water.

© 2016 Elsevier B.V. All rights reserved.

Flubendazole (Scheme 1) is an anti-parasitic agent used for the treatment of various human and animal helminthoses [1,2]. Recent reports suggest that FLU found an application in the cancer treatment [3]. Its mode of action involves the destruction of cytoplasmic microtubules in the intestinal or absorptive cells of the parasite [4]. Inhibition of glucose uptake and depletion of glycogen stores follow lead to death of the parasite [5]. Several analytical techniques such as fluorescence spectroscopy [6], liquid chromatography [7], and polarography [8] were applied for the determination of FLU in its pharmaceutical preparations. To the best of knowledge, the coordination behavior of FLU towards different metal ions has not been previously discussed in the literature.

Here, synthesis, spectroscopic and thermal characterization of Cu(II) complexes of FLU drug are reported both experimentally (see the supporting information for details) and theoretically [9,10] and are correlated. Theoretical calculations were carried out by Gaussian 03 [11] suite of programs. In addition, a simple and nontoxic method for preparation of CuO nanoparticles based upon the thermal decomposition of the synthesized Cu (II) complexes has been explored. The morphology has been characterized by different physical methods such as XRD and FE-SEM. Finally, the degradation of MB by the catalytic performance of CuO nanoparticles has been investigated with the aid of the ultraviolet radiation.

The binary complexes $[Cu(FLU)_2X_2]\cdot zH_2O$ (X = Cl^- (**1**), z = 4; $C_2H_3O_2^-$ (**3**), z = 1; X = ClO_4^- (**4**), y = 3) and $[Cu(NO_3)(FLU)_2(OH_2)]\cdot NO_3\cdot 2H_2O$ (**2**) were prepared (see the supporting information for details). Elemental analysis (supporting information) data are in agreement with those calculated for the suggested structures. Lower conductance values were reported for **1**, **3** and **4** (in DMF) compared with the reported values [12], while the higher one (100 $ohm^{-1}\,cm^2\,mol^{-1}$) of **2** suggests its ionic nature. IR bands observed at 3308, 1736, 1646 and 1595 cm^{-1} are assigned to $\nu(NH_{carb})$, $\nu(C=O_{carb})$, $\nu(C=O_{benzoyl})$ and $\nu(C=N)$, respectively. In complexes, the shift of $\nu(NH_{carb})$ and $\nu(C=O_{benzoyl})$ to higher values, 3374–3429 and 1636–1644 cm^{-1}, indicates that these groups remain intact. The $\nu(C=O_{carb})$ moves to lower wave numbers, which suggests its involvement in the chelation. As the effect of H-bond on the pyridine-type N is replaced by the complex formation, the position of $\nu(C=N)$ in IR spectra of FLU and its complexes is the same [13,14]. The new bands at 1388, 1347, 1301 cm^{-1} in **2** are due to $\nu_3(NO_3)$modes of NO_3^- group [15], while those at 1352 and 1573 cm^{-1} ($\Delta\nu$ = 221 cm^{-1}) are taken as evidence for the monodentate mode of the acetate group [16].

The TG curve of **1** (Fig. S1a†) shows two decomposition steps at 192 and 690 °C due to loss of hydrated $4H_2O$ + Cl and pyrolysis of two FLU molecules with overall mass amounts to 86.91% (calcd. 87.57%) and CuO + 2C as a residue [17]. For **2** (Fig. S1b†), four decomposition stages at 54, 186, 465 and 834 °C are observed. Two hydrated water molecules are desorbed in the first step. The

* Corresponding authors.
 E-mail addresses: mansour@sci.cu.edu.eg, inorganic_am@yahoo.com
(A.M. Mansour), noureta2002@yahoo.com (N.T. Abdel-Ghani).
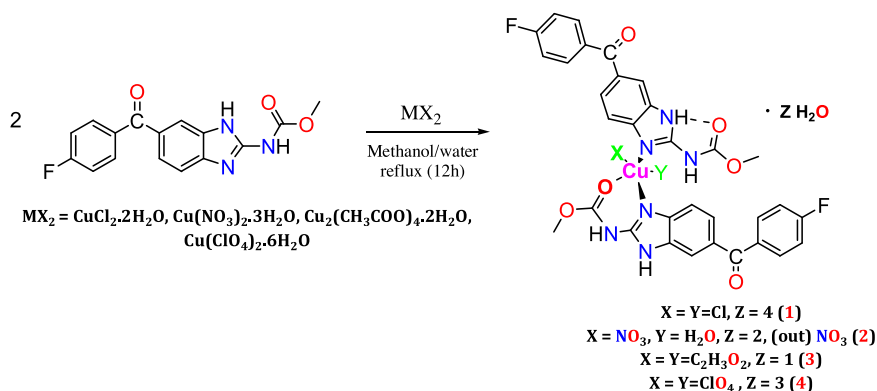
Scheme 1. Synthesis of Flubendazole-Copper(II) complexes **1**–**4**.

elimination of coordinated $H_2O + 2\,NO_3 + 2FLU$ takes place in the next stages and results in formation of Cu + CuO as a final residue, 7.86% (calcd. 8.24%). Incomplete degradation was observed in case of the acetato complex **3** (Fig. S1c†), with overall mass loss amounts to 77.76% (calcd. 88.92%), assuming the formation of CuO + C as a residue at 1000 °C. Complex **4** (Fig. S1d†) is thermally decomposed *via* five steps (49, 251, 335, 505 and 955 °C). The first step is responsible for desorption of three hydrated water molecules. The following stages give up a residue of CuO + C, 10.45% (calcd. 9.71%) through loss of two FLU and two perchlorate groups.

The observed effective magnetic moment (μ_{eff}) values, were found to be (1.80-2.06) μ_B (298 K) for the complexes (**1**–**4**). These values are expected for non-interacting Cu(II) ions (S = $^1/_2$; $t^6_{2g}e^3{}_g$), and in the acceptable range for copper complexes (1.60–2.2 μ_B) [18]. Room temperature powdered ESR spectra of **1**–**4** were recorded at X-band frequency, Fig. S2†. The chloride complex **1** shows a slightly rhombic spectrum, with three g values, $g_1 = 2.003$, $g_2 = 2.188$, $g_3 = 2.282$. The parameter R{R = $(g_2-g_1)/(g_3-g_2)$ for rhombic systems} is found to be 1.968, i.e. R > 1, which is characteristic for Cu(II) trigonal bipyramidal complexes [19]. The spectrum of **2** displays an isotropic signal with $g_{ave} = 2.131$. The ESR spectra of **3** and **4** are axial with two well-defined $g_\parallel = 1.780$, 2.073 and $g_\perp = 2.078$, 2.189, respectively and $g_\perp > g_\parallel > g_e$ (2.0023) suggesting that d_{z^2} orbital is the most populated ground state. Therefore the stereochemistry around the metal centre is proposed to be compressed trigonal bipyramidal with D_{3h} symmetry [20].

The fully optimized geometries of complexes (**1**–**4**) and the numbering of atoms are shown in Fig. 1. The atomic coordinates are

presented in Table S1. Complexes (**1**–**4**) adopt distorted trigonal-bipyramidal geometry. The basal plane is defined by carbamate oxygen atom [Cu—O(34) = 2.306 Å (**1**); 2.174 Å (**2**); 2.326 Å (**3**); 2.142 Å (**4**)] and two chlorine atoms [Cu—Cl(66) = 2.413 Å and Cu—Cl(67) = 2.267 Å] (**1**), two acetate groups [Cu—O(44) = 1.915 Å and Cu—O(45) = 1.946 Å] (**3**) or two perchlorate groups [Cu—O (44) = 2.164 Å and Cu—O(45) = 1.963 Å] (**4**). In case of **2**, three oxygen atoms; monodentate nitrate ligand [Cu—O(44) = 1.955 Å], water [Cu—O(45) = 2.137 Å] and carbamate group [Cu—O (34) = 2.174 Å], constitute the basal plane of the metal center. In each complex, the axial positions are occupied by two pyridine-type nitrogen atoms [Cu—N(10) = 1.997 Å (**1**), 1.973 Å (**2**), 2.059 Å (**3**), 1.967 Å (**4**); and Cu—N(15) = 2.032 Å (**1**), 1.977 Å (**2**), 2.085 Å (**3**), 2.009 Å (**4**)]. The N(10)—Cu—N(15) angle somewhat deviates from the linearity and is equal 168.8, 172.4 and 171.2 °for **1**, **2** and **4**, respectively. This deviation leads to formation of an irregular structure. According to NBO analysis, the electronic arrangement of Cu(II) in complex **1** is [Ar]4s$^{0.39}$3d$^{9.18}$4p$^{0.48}$5p$^{0.01}$. The occupancies of Cu 3d are: $d_{xy}$$^{1.954}$$d_{xz}$$^{1.759}$$d_{yz}$$^{1.891}$$d_{x^2-y^2}$$^{1.608}$$d_{z^2}$$^{1.973}$. For **2**, and **3**, the electronic configurations of Cu atom in **2** and **3** are [Ar] 4s$^{0.32}$3d$^{9.14}$4p$^{0.36}$and [Ar]4s$^{0.35}$3d$^{9.15}$4p$^{0.35}$5p$^{0.01}$, respectively. For complex **4**, the electronic arrangement of Cu is [Ar] 4s$^{0.31}$3d$^{9.14}$4p$^{0.37}$5p$^{0.01}$, distributed as 18 core electrons, 9.825 valence electrons (on 4s, 3d, and 4p atomic orbitals) and 0.012 Rydberg electrons (mainly on 5p orbital). The second order interaction energy (E^2) values [21,22], for **1**, are 0.46, 0.09, 0.10, 0.29 and 0.18 Kcal mol^{-1} for LP(1)N10 → RY*(5)Cu, LP(1)O34 → RY*(4) Cu, LP(1)Cl67 → RY*(2)Cu, LP(1)N15 → RY*(5)Cu and LP(1)Cl66 →
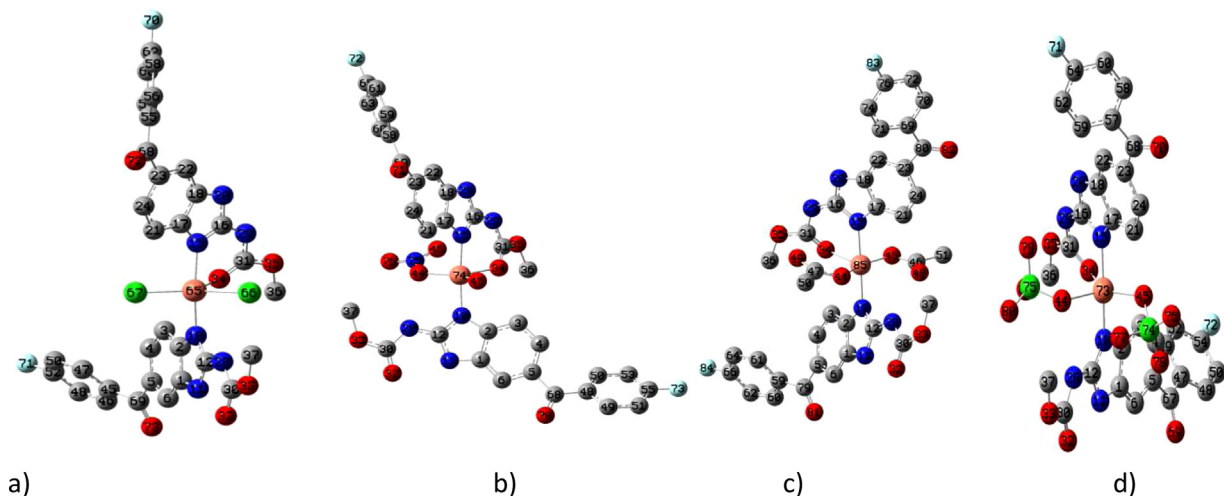

Fig. 1. Local minimum structures of complexes (a) **1**, (b) **2**, (c) **3**, and (d) **4** obtained at the DFT/B3LYP level of theory.